ALOS-2 contributions for detection of crustal deformation associated with earthquakes

*Yuji Miura[1], Basara Miyahara[1], Hiroyuki Nakai[1], Masaki HONDA[1], Yasuaki Kakiage[1], Satoshi Fujiwara[1], Hiroshi Yarai[1], Tomokazu Kobayashi[1], Yu Morishita[1]

1. GSI of Japan

Analysis of SAR images is a powerful and unique remote sensing technique for detecting coseismic crustal deformation of earthquakes with spatially high resolution and without any ground based observation infrastructures.
Advanced Land Observing Satellite 2 (ALOS-2) is an L-band synthetic aperture radar (SAR) satellite, launched by Japan Aerospace Exploration Agency (JAXA) on 24 May, 2014. Observation capability of ALOS-2 is higher than that of ALOS, the predecessor of ALOS-2 and operated from 2006 to 2011, in terms of a revisit cycle (ALOS-2: 14 days, ALOS: 46 days) and attainable spatial resolution (ALOS-2: 3 m, ALOS: 10 m). Moreover, ALOS-2 can observe not only by common right-looking but also by left-looking, and ScanSAR interferometry is always applicable, unlike ALOS. These improvements enhances rapid-response after earthquake and detection capability of crustal deformation.
SAR Analysis Working Group of the Coordinating Committee for Earthquake Prediction is a group of experts which was established under the Coordinating Committee for Earthquake Prediction, Japan, in order to detect detailed coseismic crustal deformation through analyses of SAR images of ALOS-2, develop related techniques, solve seismogenic mechanism from the deformation field and seek ways to utilize SAR data for disaster response and mitigation. The Geospatial Information Authority of Japan (GSI) is serving as the Secretariat of the working group and summarizing activities of the WG to a report which consists of results of ALOS-2 analysis, contributions for monitoring earthquakes and research regarding three years of ALOS-2 operation.
In this paper, we will show ALOS-2 contributions based on SAR interferograms of significant earthquakes which were observed by ALOS-2 upon urgent requests from the WG and analyzed by GSI. Especially in 2016, detailed crustal deformations were detected along with several inland earthquakes including the 2016 Kumamoto earthquake and the earthquake of the Central Tottori (Mj6.6). We will show SAR ingerferograms and crustal deformation fields of these earthquakes.

Keywords: ALOS-2, SAR, Earthquake, Crustal deformation

Postseismic Deformation following the 1995 Kobe, Japan, Earthquake Detected by Space Geodesy

*Manabu Hashimoto[1], Taku Ozawa[2], Takuya NISHIMURA[1], Hiroshi Munekane[3], Mikio Tobita[4]

1. Disaster Prevention Research Institute, Kyoto University, 2. National Research Center for Earth Sciences and Disaster Resilience, 3. Geospatial Information Authority, 4. Japan Aerospace Exploration Agency

A Mw 6.8 earthquake hit the city of Kobe, southwest Japan, and its surrounding area on January 17, 1995, and claimed more than 6,400 fatalities. The source faults, trending in the NE-SW direction, are estimated beneath the foothill of the Rokko Mountains, which are located north of the city and the highest peak is 931 m high, but it has a dominant right lateral strike slip components. The Rokko Mountains may have been built by the motion of active faults, but the uplift during the 1995 earthquake may not be enough. Therefore there is a possibility that postseismic deformation contributes to the building of the Rokko Mountains.

In order to study the postseismic deformation following the Kobe earthquake, we collected all available space geodetic data during about 20 years, including ERS-1/2, Envisat, JERS-1, ALOS/PALSAR and ALOS-2/PALSAR-2 images and continuous GPS data, and reanalyzed them. Especially, temporal continuous GPS observation made by the Geographical Survey Institute (present the Geospatial Information Authority), Japan in and around the Kobe area is important. We recalculated coordinates of these continuous GPS stations with recent PPP procedure using reanalyzed orbits and clocks of satellites. We made DInSAR and PSInSAR analyses of SAR images using ASTER-GDEM ver.2 or GSI DEM.

Time series analysis of JERS-1 images revealed line-of-sight (LOS) decrease of the Rokko Mountains. PSInSAR results of ALOS/PALSAR also revealed slight uplift north of the Rokko Mountains that uplifted by 20 cm coseismically. These observations suggest that the Rokko Mountains might have uplifted during the postseismic period.

LOS increase in a wedge shaped region between two active faults east of the Rokko Mountains in the vicinity of the NE terminus of the source fault of the Kobe earthquake. The LOS increase is also confirmed by ERS-1/2, Envisat and ALOS/PALSAR images. These facts indicate that the subsidence between these two faults continued up to 2010. Continuous GPS observation during the first two years of the postseismic period shows north-south extension with right lateral motion between these two faults.

These observations suggest that the Rokko Mountains may have uplift till 2010. On the other hand, active faults near the NE terminus continued to slip with the formation of graben-like structure, due to coseismically loaded stress.

Keywords: 1995 Kobe earthquake, Postseismic deformation, GPS, SAR interferometry, Rokko fault zone

Detection of both icecap and crustal deformation associated with the 2014-2015 Bárðarbunga rifting episode

*Yuji Himematsu[1], Masato Furuya[1]

1. Graduate School of Science, Hokkaido University

The 2014-2015 Bárðarbunga rifting episode is one of the largest event in Iceland. Previous studies have already reported that the earthquake swarm migrated from Bárðarbunga to Holhraun where the fissure eruptions occurred at northern edge of Vatnajökull icecap. There were few ground-based GPS observation points near the epicenters of the swarm. While the nearby crustal deformation associated with the episode have also been detected by using satellite InSAR-data, phase decorrelation problems have hampered detecting the icecap deformation during the rifting episode. Although the icecap has been known to flow steadily, one of our motivations is to see if the rifting episode affected the flow speed of ice in light of the well-known Jökulhlaups event by subglacial eruption. Moreover, phase-based InSAR measurement does not allow for the detailed measurement of the subsidence over the graben, which is indispensable to constrain the volume and geometry of intruded dike.

In this study, we processed COSMO-SkyMed images to simultaneously detect both the flow signals on the icecap and the crustal deformation associated with the rifting event. The offset tracking data derived from COSMO-SkyMed images showed the displacement signals that consist of both the crustal deformation over land and the icecap flow. Two displacement discontinuities were detected not only on the land but also on the icecap, while we could not capture the entire image of the both deformations due to the limited SAR image coverage. The 3D displacements revealed a graben structure with over 8 m subsidence at the graben floor. At the graben floor, approximately 1 m of the rift-parallel motion which caused by the dog-bone seismicity was detected. Using these observation results, we will estimate the dike intrusion model and discuss the possible interaction between the ice and the crustal deformation during the 2014-2015 Bárðarbunga rifting episode.

Keywords: Dike intrusion episode, Divergent plate boundary, Synthetic Aperture Radar, Iceland, Pixel offset technique

Crustal deformation of the 2016 October 21th M 6.6 earthquake in central Tottori prefecture.

*Takuya NISHIMURA[1], Manabu HASHIMOTO[1], Yoshinobu HOSO, Hiromu SAKAUE[2], Yuji ITOH[2]

1. Disaster Prevention Research Institute, Kyoto University, 2. Graduate School of Science, Kyoto University

Introduction

There is a zone of active microseismicity along the Japan Sea coast in the San’in region. Some large earthquakes including the 1943 M7.2 Tottori and the 2000 M7.3 western Tottori earthquakes also occurred in this seismic zone. Nishimura et al.(2014) showed a zone of high strain rate observed by GNSS almost overlapped the seismic zone and proposed to call it “the San’in shear zone”.

We constructed 13 continuous GNSS stations in Tottori and Okayama prefectures in late 2014 so as to clarify a detailed distribution of the San’in shear zone. These stations constitute three linear arrays across the shear zone. An M_{JMA} 6.6 earthquake hit central Tottori prefecture on October 21, 2016. Our GNSS network, as well as GEONET revealed a detailed pattern of crustal deformation before, during, and after the earthquake. We report the deformation observed by GNSS and InSAR.

Preseismic deformation

Deformation in the San’in shear zone is characterized by right-lateral shear movements. GNSS stations along the Japan Sea coast moves eastward relative to those in Okayama prefecture. The 20-km-wide shear zone extends in an east-west direction and accommodates 5 mm/yr of shear movements. The M6.6 earthquake occurred in the shear zone.

Coseismic deformation

Coseismic displacement was observed at GNSS stations in Tottori and Okayama prefectures (Figure). The largest displacement was observed at KRNS and shows horizontal displacement of 9 cm toward east-southeast and subsidence of 4 cm. We estimate parameters of a rectangular fault model using the observed displacement. The estimated parameters suggest a vertical fault oriented NWN-SES with left-lateral strike slip, which is concordant with aftershock distribution. The estimated moment magnitude is ~6.2. SAR interferograms of ALOS-2 show a clear quadratic pattern of surface coseismic displacement.

Postseismic deformation

Postseismic displacement at GNSS stations reached 2 cm as of end of December, 2016. Although a spatial pattern of postseismic displacement is similar to that of the coseismic displacement, observed postseismic displacement is concentrated near the source fault. It suggests shallow afterslip along the coseismic fault.

Keywords: Crustal deformation, GNSS, InSAR, San'in shear zone

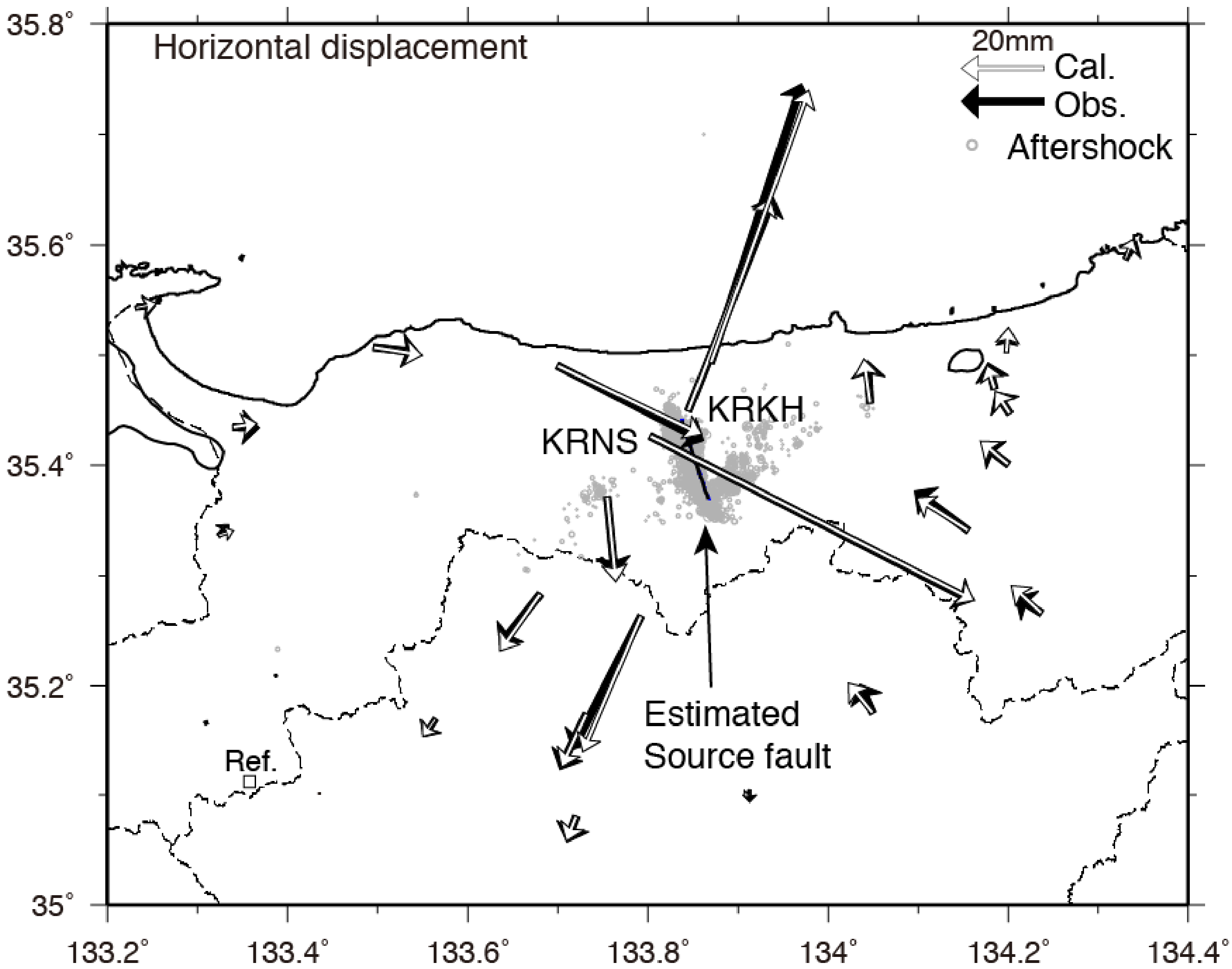

Horizontal displacement
20mm
Cal.
Obs.
Aftershock
KRKH
KRNS
Estimated
Source fault
Ref.
35.8°
35.6°
35.4°
35.2°
35°
133.2°
133.4°
133.6°
133.8°
134°
134.2°
134.4°

Post-seismic deformation of 2016 Kumamoto Earthquake by continuous GNSS network

*Shigeru Nakao[1], Takeshi Matsushima[2], Takao Tabei[3], Makoto OKUBO[4], Tadashi Yamashina[4], Takahiro Ohkura[5], Takuya NISHIMURA[6], Takuo Shibutani[6], Masahiro Teraishi[6], Takeo Ito[7], Takeshi Sagiya[8], Kenjiro Matsuhiro[7], Teruyuki Kato[9], Jun'ichi Fukuda[9], Atsushi Watanabe[9], Satoshi Miura[10], Yusaku Ohta[10], Tomotsugu Demachi[10], Hiroaki Takahashi[11], Mako Ohzono[11], Teruhiro Yamaguchi[11], Kazumi Okada[11]

1. Department of Earth and Environmental Sciences, Graduate School of Science and Engineering, Kagoshima University, 2. Institute of Seismology and Volcanology, Faculty of Sciences, Kyushu University, 3. Department of Applied Science Department, Faculty of Science, Kochi University, 4. Kochi Earthquake Observatory, Faculty of Science ,Kochi University, 5. Aso Volcanological Laboratory, Institute for Geothermal Sciences, Graduate School of Science, Kyoto University, 6. Disaster Prevention Research Institute, Kyoto University, 7. Earthquake and Volcano Research Center, Graduate School of Environmental Studies, Nagoya University, 8. Disaster Mitigation Research Center, Nagoya University, 9. Earthquake Research Institute, University of Tokyo, 10. Research Center for Prediction of Earthquakes and Volcanic Eruptions, Graduate School of Science, Tohoku University, 11. Institute of Seismology and Valcanology, Graduate School of Science, Hokkaido University

The 2016 Kumamoto Earthquake (M 7.3) attacked to Kumamoto prefecture in Japan on April 16, 2016. Seismic intensity 7 was observed twice in the 2016 Kumamoto Earthquake. Post-seismic deformation was observed after the large earthquake occurred in land and trench. Twenty-one continuous GNSS observation sites were occupied after the 2016 Kumamoto Earthquake to observed post-seismic deformation. Thirteen of our twenty-one sites were near Futagawa and Hinagu fault zones, four of our sites were around Aso Volcano, which is east from Futagawa fault zones and the others were in Ohita Prefecture, which is east of Kumamoto Prefecture

Bernese GNSS Software Ver. 5.2 is used for GNSS data analysis of our newly sites together with GEONET and JMA GNSS sites for volcanoes in Kyushu for the period from April 15 to December 31, 2016. We used CODE precise ephemerides and CODE Earth rotation parameters. The coordinates of the GNSS sites are estimated respect to ITRF2008.

Large post-seismic deformation in horizontal component was observed at CGNSS sites near Hinagu and Futagawa fault zone. However, there is almost no observation in vertical component. Largest post-seismic deformation of 11cm from April to December, 2016 is observed in NS-component at MIFN, which is located east side of Hinagu fault zone. It seems that post-seismic deformation does not come to stop. After slip model is assumed for initial post-seismic deformation from April to July, 2016. We assumed two faults, one is located in Futagawa fault zone and the other is Hinagu fault zone. Fault parameters of length, width, strike, dip, amount of slip, position are estimated by simulated annealing method. Top and bottom of fault plane are 0.1 to 40 km in Hinagu fault and 0.8 to 32 km in Futagawa fault. Two fault planes extended to mantle. It suggests that there are several phenomena in initial post-seismic deformation, effect of viscoelastic etc.

Keywords: Continuous GNSS observation, post-seismic deformation

Afterslip, viscoelastic relaxation, poroelastic rebound: A possible mechanism in the sort and long term postseismic deformation following the 2011 Tohoku earthquake.

*Hidayat Panuntun[1], SHINICHI MIYAZAKI[1], Yoshiaki Orihara[2]

1. Graduate School of Science, Kyoto University, 2. Department of Physics, Tokyo Gakugei University

Postseismic deformation of the Tohoku earthquake has been investigated by Ozawa et al. (2011), Wang et al. (2012), Diao et al. (2013), Sun et al. (2014), Perfettini and Avouac (2014), Shirzaei et al. (2014), Silverii et al. (2014), and Yamagiwa et al. (2015). Of these studies, Diao et al. (2013) investigated rheological model inferred from postseismic deformation of the Tohoku earthquake using 1.5 years GPS data following the mainshock. Because reliable investigation of the viscosity and its transient behavior require observation with longer time period, we build postseismic deformation model of the Tohoku earthquake using longer GPS data than that of used by previous studies and estimated the inferred rheological model. In addition, we also evaluate the possibility of the poroelastic relaxation signal due to the Tohoku earthquake.

We used observed surface deformation recorded by inland GEONET stations from 12 March 2011) to 12 October 2016 (~ 5.6 years). Afterslip model was inverted by assuming a homogeneous elastic half-space (Okada 1992). Viscoelastic relaxation due to coseismic stress change of the Tohoku earthquake is estimated using the Fortran code PSGRN/PSCMP (Wang et al. 2006). We estimated poroelastic relaxation following Gahalaut et al. (2008) and compared the result with observed ground water-level change to investigate relaxation time of poroelastic rebound.

Observed postseismic displacement for 5.6 following the mainshock show that deformation is characterized by seaward movement and is more broadly distributed than the coseismic displacement. Our model show an effective thickness of the elastic crust (D) and an asthenosphere viscosity (η) are 50 km and 5.6×10^18 Pa s, respectively. This result is consistent with most estimated viscosity in NE japan area (e.g., Rydelek and Sacks 1990; Suito and Hirahara 1999; Ueda et al. 2003; Hyodo and Hirahara 2003). Incorporating viscoelastic and poroelastic rebound in the early stage of postseismic deformation improve the agreement between predicted and observed displacement. It implies that postseismic deformation following the Tohoku earthquake is likely driven by multiple mechanism instead of single mechanism. Poroelastic relaxation is consistent with the ground water-level change during the first 140 days after the mainshock, suggesting that poroelastic rebound after the Tohoku earthquake have longer relaxation time than 60 days of poroelastic rebound following the 2000 South Iceland earthquake (Jonsson et al. 2003). Landward displacement of poroelastic rebound at offshore area indicate that this mechanism, along with viscoelastic relaxation, could have contributed to the postseismic deformation of the Tohoku earthquake.

Keywords: afterslip, viscoelastic relaxation, poroelastic rebound, GNSS, Postseismic deformation

Interseismic spatiotemporal change of the crustal deformation field estimated from GNSS around western coast of Tohoku region

*mika sato[1], Mako Ohzono[2], Akiko Hasemi[1]

1. Graduate School of Science and Engineering, Yamagata University, 2. Institute of Seismology and Volcanology, Graduate School of Science, Hokkaido University

The eastern margin of Japan Sea is known as strain concentration zone from some geological and geodetic studies. Sagiya et al. (2000) found the "Niigata-Kobe Tectonic Zone (NKTZ)", which is large strain rate field along Niigata to Kobe, analyzing GEONET data observed from 1997 to 2000 in whole Japan. Their result does not indicate remarkable large strain more northern region from Niigata, although relatively large strain rate is presumed by geological long-term period around the area. In addition, Yokota and Koketsu. (2015) suggests the possibility of the occurrence of the slow slip event around large area in Tohoku region before the 2011 Tohoku-oki earthquake from GNSS data analysis. This result implies that there are some abnormal spatiotemporal changes of the crustal deformation field during interseismic period in Tohoku region. After the NKTZ detection, GNSS sites are increased and more longer data can be obtained. In order to investigate spatiotemporal changes of the crustal deformation field in the interseismic period around Tohoku region including eastern margin of Japan Sea, we analyzed GNSS data at 194 stations of the GEONET. Using the F3 daily coordinates, we prepare every two-years coordinate time series and estimated velocity at each site fitting linier, annual and semi-annual trend. Obtained velocity data resolved to the subducting direction of the Pacific plate (N22°W), and plotted to velocity profile dividing 20 km-width area to north to south. As a preliminary result, we obtained velocity profile around west coast from north Niigata to south Akita. Southern part shows remarkable velocity change corresponding to the NKTZ area, meanwhile it is not clear in northern profile. Differences among two-years velocity profiles at same area were not clear excluding the case of temporal postseismic deformation after some inland earthquakes. To discuss detailed spatiotemporal change of the crustal deformation in Tohoku, we need information of more wider area of the velocity field.

Crustal deformation in and around the Atotsugawa fault before and after the Tohoku-Oki earthquake

*Tomomi Inamatsu[1], Youichiro Takada[1], Takeshi Sagiya[2], Takuya NISHIMURA[3]

1. Graduate School of Science, Hokkaido Univ., 2. DMRC, Nagoya Univ., 3. DPRI, Kyoto Univ.

The 2011 Tohoku-Oki earthquake (Mw9.0) provides us the first opportunity to examine the responses of strain accumulation zones and active faults to megathrust earthquakes with dense permanent GPS network. In this presentation, we report the differences and/or similarities between pre, co, and post seismic crustal deformation of the Tohoku-Oki earthquake using GPS data in and around the Atotsugawa fault, located at the central part of Niigata-Kobe Tectonic Zone (NKTZ, Sagiya et al., 2000).
We used daily coordinates obtained from the GPS stations operated by university group in addition to GEONET by Geospatial Information Authority (GSI). For the pre-seismic period, we estimated the velocity field by removing annual and semi-annual components from the daily coordinates. For the post-seismic deformation, we extracted the period from 25 November 2014 to 2 July 2016, and estimated the velocity field in the same manner. For the co-seismic displacement, we calculated the average coordinates for 5 to 10 March 2011 and 12 to 17 March 2011, and subtracted the former from the latter. From the velocities and displacements thus determined, we calculated the strain rates following the method of Shen et al. (1996) with CCD of 20 km.
Spatial pattern of the co-seismic strain is completely different from the pre and post seismic strain rates pattern. The co-seismic deformation indicates elastic strain, and its spatial variation indicates heterogeneity in the elastic constants. Therefore we conclude that the pre and post seismic strain concentration is mainly caused by the inelastic straining. The strain rates before and after the earthquake are similar to each other, which can be explained by considering inelastic deformation responsible for the strain rate concentration. The inelastic strain, viscous flow for example, depends on the absolute stress accumulated over a long time scale, which is far larger than the stress change by one earthquake. The similarity in pre and post-seismic strain rates is consistent with a previous study for the northern part of NKTZ (Meneses-Gutierrez and Sagiya, 2016).
The deformation pattern before and after the earthquake are characterized by high strain rates along the Atotsugawa fault and its eastern and western ends where volcanic activity is high. In the volcanic areas, due to the high temperature, the viscous flow would be dominant. Along the Atotsugawa fault, on the other hand, the fault slip at the depth would be dominant. Thus, different mechanisms of inelastic deformation would proceed simultaneously in and around the Atotsugawa fault.
Looking in detail, we noticed some differences between pre and post-seismic strain rate pattern. For example, the sense of strain rates reversed in the south of the Hida mountain range and to the east of Mt. Ontake. Both regions are known as thermally active areas and many small earthquakes have been occurring frequently. Considering these points, the change in the strain rates in these regions are probably related to the volcanic activities.

Keywords: Tohoku-Oki earthquake, GPS, inelastic strain

Estimation of postseismic deformation at the seafloor GPS-A sites following the 2004 off the Kii Peninsula earthquakes

*Shun-ichi Watanabe[1,2], Yehuda Bock[2], Tadashi Ishikawa[1], Yusuke Yokota[1], Keiichi Tadokoro[3]

1. Hydrographic and Oceanographic Department, Japan Coast Guard, 2. Scripps Institution of Oceanograpy, 3. Earthquake and Volcano Research Center, Nagoya University

Dense near-fault GPS-A seafloor geodetic and on-shore GPS GEONET observations provide significantly improved resolution of the interseismic slip deficit in the Nankai trough, Japan [Yokota et al., 2016]. In a previous study, we included additional seafloor data at the Kumano basin collected by Nagoya University [Tadokoro et al., 2012] to estimate expected seafloor deformation during a large subduction zone earthquake as input to tsunami models [Watanabe et al., 2016 AGU]. However, in order to derive the stable velocities from GPS-A or GNSS data, the displacements caused by episodic events should be quantitatively estimated. Whereas the coseismic and postseismic deformations at the GPS-A sites associated with the 2011 Tohoku-oki earthquake had been already removed in the previous studies, the postseismic deformation of the southeastern off the Kii Peninsula earthquakes (on Sep. 5, 2004 JST, M_{JMA} 7.1, 7.4) have not been quantified. In this study, we constructed the FEM model to calculate the viscoelastic relaxation following these events. At first, we re-estimated coseismic finite fault source models, referencing the source parameters provided by Yamanaka [2004], Saito et al. [2010], Tadokoro et al. [2006] and Kido et al. [2006] for the mainshock, and those by Bai et al. [2007] and Yamanaka [2004] for the foreshock. The viscoelastic deformation was calculated using a 3D FEM model with a realistic subduction geometry. Whereas the oceanic slab and the continental lithosphere were assumed to be an elastic body, the oceanic mantle, the mantle wedge, and the weak asthenosphere which underlay the slab were assumed to have a bivisocous Burgers rheology. The displacements due to afterslip occurring around the rupture planes were also estimated to reproduce the residuals between observed and FEM-calculated viscoelastic displacements. Calculating the observation-calculated misfit values, the different parameter sets for viscosities of the mantle and the asthenosphere, and thickness of the continental lithosphere were tested. The preferred model with the lowest misfit value provided the southward displacements of up to 1 cm/year (between July 2006 and July 2009) in the Kumano Basin. Our result affects the estimation of the slip deficit rate in the Nankai subduction zone, such as provided by Yokota et al. [2016], where megathrust earthquakes have repeatedly occurred. In the presentation, we will show the possible impacts of these events and their postseismic deformation on the slip deficit estimate.

Keywords: Postseismic deformation, Finite element method (FEM) modeling, GPS-A seafloor geodetic observation, 2004 southeastern off the Kii Peninsula earthquakes, Viscoelastic relaxation

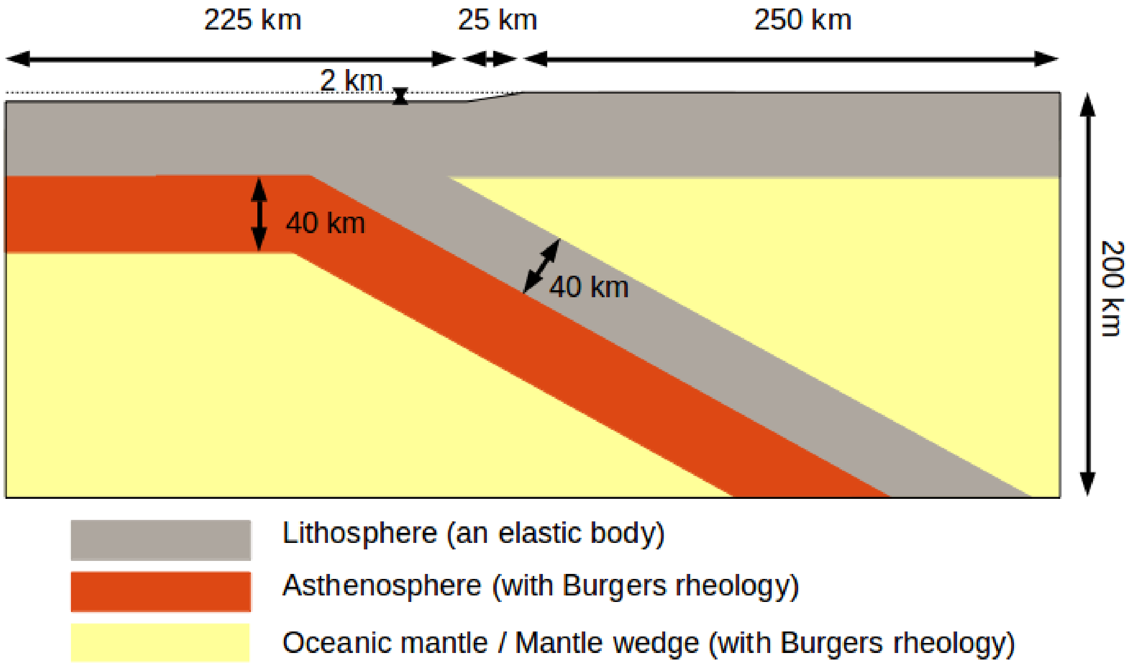

Fig. Schematic picture of FEM structure (cross section)

Vertical velocity profile and possible velocity changes in SW Japan from GNSS data over the last 20 years

*Yutaro Iwasa[1], Kosuke Heki[2]

1. Space Geodesy Laboratory, Earth and Planetary Dynamics, Natural History Sciences, Graduate School of Science, Hokkaido University, 2. Earth and Planetary Science, Graduate School of Science, Hokkaido University

GNSS (Global Navigation Satellite System) observations have been playing a major role in studying crustal deformation near plate boundaries. Such observations provide valuable information on, e.g. fault mechanisms of earthquakes, and also contribute to mitigation of volcanic disasters. In addition to them, inter-seismic crustal deformation reflect strain accumulation in the plate interface, and enables us to study mechanical coupling between the plates. So far, most of these results are based on horizontal components of the 3-D crustal deformation, and the vertical components has not been well utilized. This would be due to the lower signal-to-noise ratio of the vertical crustal movements. On the other hand, in the plate boundary region, the horizontal components include both rigid plate motion and interplate coupling. On the other hand, the vertical components only contain the latter, and directly reflect inter-plate coupling. Aoki and Scholz (2003) analyzed the vertical crustal movement of the Japanese Islands using the data over three-year period 1996-1999. We already have 20 years of crustal movement data from the Japanese dense GNSS array GEONET (GNSS Earth Observation Network), and much more accurate vertical velocity data are available. In this study, we estimated vertical velocity using the time seris 1996-2016. In particular, we analyzed the interplate coupling in Southwest Japan using the vertical velocity profile spanning from the Muroto Cape to the Oki Islands. The interplate coupling in the Japan Trench is reported to have gradually weakened over the years before the 2011 Tohoku-Oki earthquake. Classical studies of viscous flow contribution in subduction zones have also suggested that crustal deformation rate may change within an earthquake cycle. The Nankai Trough is the plate boundary where the Philippine Sea plate subducts, and the next inter-plate earthquake is anticipated to occur within the coming years or decades. With the long-term data spanning ~20 years, we could study the temporal change of the vertical velocities. Here we modeled them using quadratic functions of time, and discusss the significance of the quadratic terms. GNSS stations close to the Nankai Trough subside while those a little farther apart show uplift. Then, the temporal change in the coupling would appear in various polarities and amounts for these stations. On the other hand, if the acceleration is simply due to some unknown movement of the reference point, the quadratic term would appear as a uniform value in all the station. In this study, I compared the linear trend and the quadratic components of stations with various distances from the trench, and found that the quadratic term might be a leakage from the movement of the reference point.

Keywords: Vertical Velocity

Interseismic Strain Partitioning in Nankai Subduction Zone, Southwest Japan: Block Movement and Internal Deformation of the Forearc Sliver

*Masahiko Shiomi[1], Takao Tabei[2], Takeo Ito[3], Makoto Okubo[2]

1. Graduate School of Science, Kochi University, 2. Faculty of Science, Kochi University, 3. EVRC, Nagoya University, Nagoya, Japan

We study interseismic strain partitioning in the Nankai subduction zone, southwest Japan (SWJ). Oblique subduction of the Philippine Sea plate (PHS) and strong coupling on the plate interface have deformed the overriding SWJ arc in two ways: interseismic crustal shortening in the direction of PHS convergence and long-term lateral block movement of the forearc sliver along the Median Tectonic Line (MTL) that is the arc-parallel strike-slip fault dividing the forearc from the rest of SWJ. Slip deficit on the MTL fault plane may disturb local deformation filed.

Basic data used in this study are GPS displacement rates obtained from the nationwide continuous network. We incorporate the rates from dense campaign measurements along two traverse lines across the MTL to improve spatial resolution around it. Furthermore we add seafloor displacement rates near the Nankai Trough to better estimate plate coupling far offshore. PHS interface and MTL fault plane are reproduced by many triangular elements to a depth of 50 km and 15 km, respectively. We introduce Markov Chain Monte Carlo method to simultaneously estimate slip deficit distribution on the PHS interface and MTL fault plane, together with the Euler vector of the forearc block motion relative to SWJ.

The slip deficit rate on the PHS interface is the strongest (> 50 mm/yr) at the depth of 15-25 km, which nearly overlaps with the main rupture zone at the last megathrust event in 1946. While the slip deficit rates decrease steeply toward the deeper portion, they are still large enough in a shallower zone near the trough. Rate of the forearc block motion is 5-7 mm/yr relative to SWJ but locking of the MTL fault plane is not uniform from east to west. The block motion across the MTL and partial locking of its boundary fault plane have caused a small-scale shear deformation zone in the SWJ arc.

Keywords: Crustal deformation, Southwest Japan, Philippine Sea plate, Median Tectonic Line, GPS

Block motion model in Colombia, using GNSS Observation network (GEORED)

*Takeo Ito[1], Hector Mora Paez[2], Juan Ramor Gaviria[2], Takeshi Sagiya[3]

1. Earthquake and Volcano Research Center, Graduate School of Environmental Studies, Nagoya University, 2. Servicio Geologíco Colombiano, 3. Disaster Mitigation Research Center, Nagoya University

Introduction
Colombia is located at the boundary between South-America plate, Nazca Plate and Caribrian plate. This region is very complexes such as subducting Caribrian plate and Nazca plate, and collision between Panama and northern part of the Andes mountains. Although, the effect of subducted Caribrian plate is not clear, the previous large earthquakes occurred along the subducting boundary of Nazca plate, such as 1906 (M8.8) and 1979 (M8.2). These previous earthquakes caused huge damage to life infrastructure and also lost the life along the subduction zone. And also, earthquakes occurred inland, too. So, it is important to evaluate earthquake potentials for preparing huge damage due to large earthquake in near future.

GNSS observation
In the last decade, the GNSS observation was developed in Columbia. The GNSS observation is called by GEORED, which is operated by servicing Geologico Colomiano. The purpose of GEORED is research of crustal deformation. The number of GNSS site of GEORED is consist of 93 continuous GNSS observation site at 2016. The number of GEORED's GNSS site is increasing now. The sampling interval of almost GNSS site is 30 seconds, a part of GEORED is 1 second of sampling interval. In addition, there are campaign type of GNSS observations around the main active faults. A part of campaign type of GNSS observation was started at 1990's. These GNSS data were processed by PPP processing using GIPSY-OASYS II software. GEORED can obtain the detailed crustal deformation map in whole Colombia.

Method
We developed a crustal block movements model based on crustal deformation derived from GNSS observation. Our model considers to the block motion with pole location and angular velocity and the interplate coupling between each block boundaries, including subduction between the South-American plate and the Nazca plate. And also, our approach of estimation of crustal block motion and coefficient of interplate coupling are based on MCMC method. The estimated each parameter is obtained probably density function (PDF). This definition of crustal block model is evaluated by Akaike's information criteria (AIC).

Result
We tested 11 crustal block models based on geological data, such as active fault trace at surface. The optimal number of crustal blocks is 11 for based on geological and geodetic data. These results obtained rigid block motion model with linear problem. This model selection is based on AIC, which based on the number of parameters and residual between calculation and observation. In this presentation, we will discuss spatial interplate coupling ratio and also earthquake potential at inland faults.

Keywords: crustal block model, GNSS

Integrated analysis of GNSS data for volcano surveillances in Tohoku region, Japan

*Jun Okada[1]

1. Volcanology Research Department, Meteorological Research Institute - Japan Meteorological Agency

GNSS geodesy techniques have been widely applied for monitoring volcanic deformations in the world, for example the 2010 eruption of Eyjafjallajokull, Iceland (Sigmundsson *et al*., 2010), the 2011 caldera unrest of Santorini, Greece (Newman *et al*., 2012) and the 2011-2012 eruption crisis of El Hierro, Spain (Lopez *et al*., 2012). These case studies have deepened our understandings of magma supply system beneath volcanoes. In Japan, several institutes including Japan Meteorological Agency (JMA) has conducted GNSS surveillances in both continuous and campaign styles near active volcanoes whereas Geographical Survey Institute (GSI) has operated GEONET (e.g. Nakagawa *et al*., 2009) which are widely distributed throughout Japan archipelago and mostly located far from volcanoes. Since in many cases, GNSS data have been analyzed independently by each institute with different strategies using different reference systems, there are rooms to discuss the consistency of the solutions. In order to obtain homogeneous solutions from far field to the vicinity of volcanoes, GNSS data sets of JMA and GSI are combined and analyzed with the same parameters and strategies. It is possible to evaluate whole volcanic system consistently using the combined data set which is sensitive to both the deep and the shallow depths. Bernese 5.2 software (Dach *et al*., 2013) and IGb08 reference coordinates are used to obtain 24-hours solutions. In Tohoku region, in order to detecting volcanic signals, careful treatments are needed by properly evaluating the effects of postseismic deformation by the 2011 Tohoku Earthquake (e.g. Tobita 2016), the steady plate motions and the seasonal trends (Geirsson *et al*., 2006). The 2014-2015 volcanic activity of Azumayama on the border of Fukushima and Yamagata prefectures has been analyzed by this study.

Keywords: deformation, GNSS, volcano surveillance, postseismic deformation, Azumayama

The role of depth-dependent background crustal viscosity in volcano deformation

*Tadashi Yamasaki[1]

1. National Institute of Advanced Industrial Science and Technology

Geodetic (GPS and/or InSAR) observations have provided precise constraints on the mechanism that drives volcanic crustal deformation. Viscoelastic relaxation may play an important role in a long-term component of the deformation because in volcanic region the crustal viscosity is likely weakened by high geothermal gradient. A model with spatially uniform viscosity may be reasonably simple to examine the response of viscoelastic crust in a first-order approximation. But, in more detail, the crustal viscosity spatially varies in rich variety of ways, but the variation with depth is probably the most essential on which further variation would be superimposed, because the crust constitutes a part of the thermal boundary layer in which temperature increases with depth. This study investigates the role of depth-dependent viscosity (DDV) structure in viscoelastic crustal deformation by magmatic intrusion.

The linear Maxwell viscoelastic response of the crust and mantle to the inflation of a magmatic sill is solved, using a parallelized 3-D finite element code, OREGANO_VE [e.g., Yamasaki and Houseman, 2015, J. Geodyn., 88, 80-89]. The viscoelastic crust has depth-dependent viscosity (DDV) structure; the viscosity hc exponentially decreases with depth: hc = h0 exp[c(Zc - z)/L0)], where h0 is the viscosity at the bottom of the crust, c is a constant; c > 0 for DDV model but c = 0 for uniform viscosity (UNV) model, Zc is the thickness of the crust, z is the depth and L0 is a reference length-scale. The viscoelastic mantle has spatially uniform viscosity hm. For UNV model, so high viscosity is given to the uppermost layer with a thickness of H that it deforms in elastic fashion. DDV model however avoids having such an artificial elastic layer. The sill inflation is introduced by using the split node method developed by Melosh and Raefsky [1981, Bull. Seism. Soc. Am., 71, 1391-1400]. The geometry of the sill is approximated as an oblate spheroid whose depth is D, equatorial radius is W and thickness at the centre is dc. The inflation occurs instantaneously at time t = 0.

UNV model (c = 0) behaviour shows that an inflation-induced surface uplift abates with time by means of viscoelastic relaxation, whose subsidence rate is higher and slower if the sill is inflated at deeper in elastic and viscoelastic layer, respectively, and accordingly maximised by the inflation at the boundary between elastic and viscoelastic layers. The rate also depends on the artificially assumed elastic layer thickness H. DDV model (c > 0), on the other hand, shows that for a given c the subsidence rate is greater for greater D, which reflects the viscosity variation with depth. The available magnitude of the subsidence is greater for greater c, which is consistent with the UNV model behaviour that the subsidence is smaller for smaller H. Even if the viscosity gradient is very small, however, the model, having W and D being relatively small to a length-scale over which the viscosity decreases with depth, enhances the rate and available magnitude of subsidence as if the elastic layer is effectively thickened.

The DDV model behaviour requires an effective elastic thickness (EET) to be constrained for a given viscosity gradient in order to properly evaluate the deviation from UNV model behaviour. We thus in this study constrain EET by applying a UNV model behaviour that the post-inflation subsidence rate is slower for a deeper inflation if the inflation occurs in the viscoelastic layer. The DDV model is compared with a UNV model with H = EET, showing that at each surface point the UNV model approximates DDV model behaviour to some extent, but the apparent UNV which best fits the DDV model displacement history is smaller at greater distance from the centre of the uplift and that DDV model displacement is characterised by higher viscosity later in post-inflation period.

A new form of the equation system for geodyamics with clear and solid physical basis

*Taroh Matsuno[1]

1. Japan Agency for Marine-Earth Science and Technology

As the equation system for describing dynamical phenomena of the solid interior of the Earth such as mantle convection, plate tectonics and their interaction and so on, the equation system for Maxwellian viscoelastic media has been adopted so far. However, the idea that the interior of the earth behaves as a viscous fluid on long time-scales (e. g. Turcotte and Schubert, 2002) cannot be accepted from the simplest physical viewpoint that rocks are elastic solids in the usual sense of physics. Their dynamics must obey physical law of elastic solids regardless of time-scales. The origin of regarding long time-scale evolution of the solid earth as that of a viscous fluid might be similarity between creep of solids (including rocks) and motion of viscous fluids (e. g. McKenzie, 1967). However, creeping occurs as a result of transformation of temporal elastic strain into plastic permanent strain, often referred to as (elastic) stress relaxation. This is a physical process other than dynamical force balance, and hence it must be included in the basic equation system for geodynamics separately from the equation of motion. In the equation of motion, elastic force balances with other forces on long time-scales, where no viscous force is working. Starting from this system of two equations resultant mathematical expression becomes very similar to the equation of motion of viscous fluids if the rate of plastic displacement is identified with fluid velocity. Even with this similarity in recent numerical simulation studies treating mantle convection and plate motion together, in which fundamental unknown variable is fluid velocity, it is pointed out that behaviors of solid plates are not well simulated. In the proposed new form of basic equations the dynamical balance (equation of motion) is that of elastic solid so that this difficulty must be avoided. Further, in the new form dynamics equation is the one for elastic solid so that it can be extended to include brittle feature of the solid to generate fractures, i. e., earthquake and faulting. Thus new form of the basic equation system can be common basis for such important challenges in geodynamics.

Keywords: geodynamics, mantle convection and plate motion, Maxwellian viscoelastic media

Permeability heterogeneous structure nearby a fracture zone estimated by observed groundwater migration

*Atsushi Mukai[1], Shigeaki Otsuka[2], Yoichi Fukuda[3]

1. Fukuyama City University, 2. Kobe Gakuin University, 3. Graduate School of Science, Kyoto Univ.

Permeability structure in a fault fracture zone might change due to seismic motion. However we have not realized the spatial scale of the change definitely. In this study, we observed pore pressure changes due to seismic motions at three sites in Rokko-Takao station which was established in a tunnel penetrating the fracture zone of Manpukuji fault, and estimated local changes in permeability structure nearby the fault fracture zone.
Groundwater migration is considered to mainly occur in a fracture zone, because permeability in that area is higher than the surrounding crust. Therefore, a fault fracture zone is approximately assumed to be one board with homogeneous permeability. Mukai et al.(2015) made a one-dimensional groundwater migration model and derived the method to estimate change in permeability by using changes in groundwater discharge and pore pressure. When we applied this model to the data obtained at Rokko-Takao station, we found that permeability in the fault fracture zone had been reduced during a few months just after the 2011 off the Pacific coast of Tohoku Earthquake. This result shows that a strong seismic motion propagated from a long distance could affect permeability structure in a fault fracture zone even though the fault was not an earthquake source fault.
To investigate the spatial distribution of groundwater migration, we newly installed two pore pressure meters in addition to the existing instruments in 2016. When we estimated permeability changes by using the observational data of pore pressure and groundwater discharge, we found that the permeability structure had changed just after the 2016 Kumamoto earthquake and the 2016 central Tottori earthquake as well. However the permeability changes depended on the location to observe the pore pressure, or the distance from the fault. For instance, just after the 2016 Kumamoto earthquake, permeability close to the fault rose by about 7%, while one in dozens of meters distance reduced by about 22%. This discrepancy might be caused by the outflow of mud due to the seismic motion. In the undeveloped fracture zone apart from the fault, the mud could be blocked and the permeability might be reduced, while the mud could flow out in the completely developed fracture zone nearby the fault.

Keywords: fault fracture zone, permeability structure, 2016 Kumamoto earthquake

